



Identifying potential biological processes and key targets in COVID-19-associated heart failure

Jia Li^a, Zhifu Guo^{a,*}, Xiaowei Song^{a,**}

^a Department of Cardiology, Changhai Hospital, Naval Medical University, Shanghai, China

ARTICLE INFO

Keywords:
 COVID-19
 Heart failure
 Key genes
 WGCNA
 Bioinformatics

ABSTRACT

Novel coronavirus pneumonia (COVID-19) is a new type of viral pneumonia caused by severe acute respiratory syndrome coronavirus 2 (SARS-CoV-2) that has spread rapidly and become a global pandemic. Heart failure (HF) is the ultimate period of the development of various cardiovascular diseases. There are several research have found that SARS-CoV-2 infection may induce cardiac complications including enhanced cardiac stress biomarkers and heart failure. Our research aims at identifying underlying biological processes and key targets in COVID-19-associated heart failure via bioinformatics analysis. A total of three heart failure datasets and three COVID-19 datasets were obtained using the Gene Expression Omnibus (GEO) database. Batch effects cross each sample were eliminated with surrogate variable analysis algorithm. Then, we identified key modules of COVID-19 datasets and heart failure datasets through weighted gene co-expression network analysis. HF-associated as well as COVID-19-associated key modules were intersected for determining the shared genes of COVID-19-associated heart failure. The pivotal genes associated with COVID-19-related heart failure were determined by intersecting the shared genes with the HF-associated hub genes selected through WGCNA. Furthermore, we conducted GO as well as KEGG enrichment analysis on shared genes of COVID-19-associated heart failure. Two COVID-19-associated key modules as well as three HF-associated key modules were determined. In addition, eleven shared genes for COVID-19-associated heart failure were determined. In conclusion, our work screened two critical genes, namely PYGM and BLM, which may be possible intervention targets for COVID-19-associated heart failure. According to functional enrichment results, the shared genes of COVID-19-associated heart failure showed high enrichment in starch and sucrose metabolism, homologous recombination, Fanconi anemia pathway, and insulin resistance indicate the probably biological processes linked to COVID-19-associated heart failure. These results provided further insights in possible interventional and therapeutic targets of COVID-19-associated heart failure.

1. Introduction

Severe acute respiratory syndrome coronavirus 2 (SARS-CoV-2), which causes coronavirus disease 2019 (COVID-19) that has

Abbreviations: GEO, Gene expression omnibus; GO, Gene ontology; KEGG, Kyoto Encyclopedia of Genes and Genomes; WGCNA, Weighted gene co-expression network analysis; PPI, Protein-protein interaction; HF, heart failure.

* Corresponding author.

** Corresponding author.

E-mail addresses: 13918459432@163.com (Z. Guo), xiao_wei_song@163.com (X. Song).

<https://doi.org/10.1016/j.heliyon.2023.e18575>

Received 7 March 2023; Received in revised form 14 July 2023; Accepted 20 July 2023

Available online 25 July 2023

2405-8440/© 2023 The Authors. Published by Elsevier Ltd. This is an open access article under the CC BY-NC-ND license (<http://creativecommons.org/licenses/by-nc-nd/4.0/>).

spread rapidly and reached a pandemic level [1]. Acute respiratory infections, particularly influenza and respiratory syncytial virus are recognized causes for cardiovascular disease (CVD) [2,3]. Underlying cardiovascular disease is commonly related to comorbidities, which may increase the morbidity and severity of infectious diseases [4]. Several epidemiological studies have found that patients with comorbidity cardiovascular disease (CVD) have a higher rate of progression and mortality than those people without CVD after diagnosis of COVID-19 [5]. There is increasing evidence that SARS-CoV-2 infection may induce cardiac complications including enhanced cardiac stress biomarkers, heart failure, and arrhythmias [6]. Heart failure (HF) is the ultimate period of the development of various cardiovascular diseases. New or existing heart failure in the setting of COVID-19 can present a set of unique challenges [7]. Respiratory infections are the most common cause of heart failure [8]. There are probably a variety of pathophysiological mechanisms contributing to COVID-19-associated heart failure. However, the possible biological processes in COVID-19-associated heart failure remains unclear. Nowadays, our knowledge of COVID-19 is still evolving rapidly, and this study discusses underlying biological processes and key targets in COVID-19-associated heart failure, contributing to further insight into possible interventional and therapeutic targets of COVID-19-related heart failure.

The SVA package [9] includes functions for eliminating batch effects and other unrequired variations in high-throughput experiments. In particular, the SVA package contains functions for identifying and building directly surrogate variables from high-dimensional data (like RNA sequencing, gene expression, methylation data) that can be applied to subsequent analyses to adjust for unmodelled, unclear, or underlying noise sources [9]. Removing batch effects and utilizing surrogate variables in differential expression analysis has been demonstrated to stabilize error rate estimates, increase repeatability, and decrease dependence [10–12].

The analysis of gene differential expression typically greater focus on respective genes expression impacts, whereas neglecting the interactions among genes in intricate biological gene networks, also without establishing the connection between genes as well as diseases. However, we can employ weighted gene co-expression network analysis (WGCNA) [13] to address the problems. WGCNA is a biological method for analyzing gene expression patterns of multiple samples, which can assess the interaction between specific features, genes, and modules, as well as gives deep insights of low-expressed variation genes, and eventually identifying potential biological processes and crucial genes [14]. In this present study, the gene expression network, which follows a scale-free distribution was constructed by applying the WGCNA algorithm. Then, we established a hierarchical clustering tree via calculating the dissimilarity coefficients of different nodes. In addition, we classified genes with high similarity into the same type modules and genes with low similarity into the modules of different types as well as visualized the modules. In our study, bioinformatics analysis of transcriptome sequencing was performed to reveal the key genes of COVID-19-associated heart failure in patients, offering novel insights into the diagnosis and treatment of the disease.

2. Methods

2.1. Data source and processing

The Data source were showed in Table 1. The design of this study design is illustrated, as shown in Fig. 1. Three COVID-19-associated expression information were downloaded from the GSE156754, GSE169241, GSE151879 datasets exploiting the GEO public database (<https://www.ncbi.nlm.nih.gov/geo/>), of which the GSE156754 dataset had 9 COVID-19 cases and 3 normal samples; GSE169241 dataset had eight samples (COVID-19: Normal = 3:5); GSE151879 dataset had twelve samples (COVID-19: Normal = 1:1). Three heart-failure-related raw sequence data were downloaded from the GSE46224, GSE116250, GSE135055 datasets, of which the GSE46224 dataset had 31 heart failure cases and 8 normal samples; GSE116250 dataset had 50 heart failure cases as well as 14 normal samples; GSE135055 dataset included 21 heart failure cases and 9 normal samples. To obtain expression matrices, raw sequence data from three heart failure GEO datasets were processed with the following steps: (1) Reads with average quality score less than Q20 and a length <36 bp were removed with fastp (version 0.23.2) [15] to obtain high-quality reads; (2) Sample quality results were assessed and aggregated with FastQC (version 0.11.7) [16] as well as MultiQC (version 1.13) [17]. (3) The clean reads were then aligned against the human reference genome hg38 using STAR (version 2.7.9) [18]. (4) The gene counts of mapped reads were summarized with featureCounts (version 2.0.1) [19]. (5) The Entrez IDs of gene expression matrix were reannotated to gene symbols using the org.Hs.eg.db (version 3.15.0) [20] package for subsequent analysis.

2.2. Elimination of batch effects

For batch effects, the surrogate variable analysis (SVA, version 3.44) [9] method was used to remove batch effects between each

Table 1
Details for GEO datasets.

Number	Condition	GEO Accession	Number of samples	Platform
1	COVID-19	GSE156754	12	GPL18573
2	COVID-19	GSE169241	8	GPL24676
3	COVID-19	GSE151879	12	GPL18573
4	Heart Failure	GSE46224	39	GPL11154
5	Heart Failure	GSE116250	64	GPL16791
6	Heart Failure	GSE135055	30	GPL16791

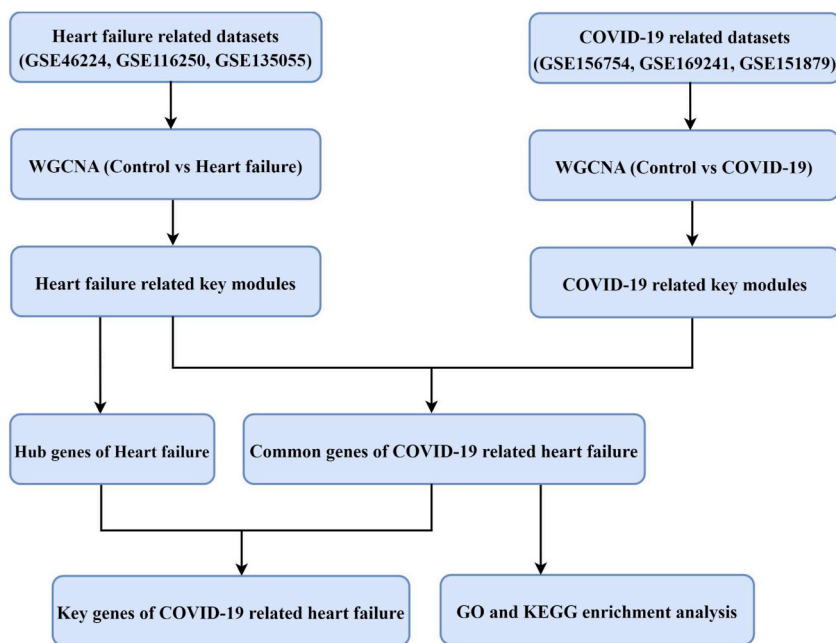


Fig. 1. The process of data preparation and analysis. WGCNA: weighted gene co-expression network analysis.

sample. The results before and after elimination of batch effects for each sample in the COVID-19 as well as heart failure datasets were represented via PCA graph. Subsequently, the common genes from the three COVID-19 expression matrices were combined into a new gene expression profile. The heart failure datasets were merged, the shared genes from the three datasets were gathered to form a novel gene expression matrix.

2.3. WGCNA construction and disease-associated key module recognition

WGCNA R package (version 1.71) [13] was utilized to construct a co-expression network by considering the gene expression profile previously obtained as input expression information and HF or COVID-19 and normal as trait information. Initially, samples were clustered to detect outliers by the `hclust` function, and the method parameter was configured to "average" for calculating the distance. Next, the `pickSoftThreshold` function was performed to determine the approximate soft threshold (β) for scale-free topology analysis. Additionally, adjacency matrix was obtained using adjacency function. Further, the adjacency matrix was converted to topological overlap matrix performing the TOMsimilarity function. The topological overlap matrix was hierarchical clustered using dissimilarity between genes, and then the tree was divided into separate modules using the dynamic shear tree method. Moreover, the `moduleEigengenes` function was utilized to determine module eigengene values. Pearson correlation analyses were used between the traits of samples and the module eigengene values of blocks. Eventually, the modules with correlation coefficient >0.4 and P values <0.05 were identified as COVID-19- or heart failure-related key modules. The hub genes of key blocks were screened according to the following criteria: (1) Gene Significance (GS) within the genes and trait >0.2 ; (2) Module Membership (MM) value >0.8 ; (3) weighted correlation <0.01 .

2.4. Identification of common and key genes in COVID-19-associated heart failure

The shared genes of COVID-19-associated heart failure was determined via overlapping COVID-19-associated key modules with HF-associated key modules. Besides, the STRING website (<https://cn.string-db.org/>) was utilized for constructing its protein-protein interaction (PPI) network with a confidence level of 0.4. Further, we imported the relationship pairs into Cytoscape (version 3.9.1) [21] software for visualization and selected out hub nodes with a high degree of connectivity as hub genes of heart failure-associated key modules in the network. The key genes of COVID-19-associated heart failure were determined via intersecting shared COVID-19-associated heart failure genes and heart failure-associated hub genes.

2.5. Functional enrichment of common genes in COVID-19-associated heart failure

The `org.Hs.eg.db` (version 3.15.0) [20] and `clusterProfiler` (version 4.4.4) [22] R packages were applied for GO as well as KEGG enrichment analyses of shared genes in COVID-19-associated heart failure. The cutoff for determining significant enrichment was set with P value <0.05 . The top twenty GO as well as top ten KEGG signaling pathways were visualized with the `dotplot` function of the R package.

3. Results

3.1. Construction of WGCNA

The surrogate variable analysis algorithm was utilized to eliminate batch effects in COVID-19 as well as heart failure datasets, as displayed in Fig. 2A–D. We performed WGCNA to determine co-expressed gene modules for the COVID-19- and heart failure-associated datasets. The scale-free topological index was 0.75 and 0.8 while the soft threshold values regarding COVID-19 and heart failure were 12 as well as 16, separately, as determined from Fig. 3A and B. Consequently, the two networks both follow a power-law distribution. The dynamic shear tree algorithm was performed to segment the modules with the set min module size of 30 to get eight modules and eleven modules for the COVID-19 and heart failure datasets, respectively. (Fig. 3C and D).

3.2. Disease-associated key module identification

In view of the hierarchical clustering and Person correlation analyses, the most relevant modules to disease were identified. The correlation between module eigengene values and traits showed that the green ($r = 0.59$, $P = 4E - 04$) and red ($r = -0.5$, $P = 0.003$) modules were deeply connected with COVID-19, whereas black ($r = 0.72$, $P = 9E - 22$), green (-0.59 , $P = 2E - 13$) and purple (-0.43 , $P = 4E - 07$) modules were markedly correlated with heart failure (Fig. 4A and B). Thus, the green and red modules were identified as COVID-19-associated key modules, and the black, green as well as purple blocks were determined as heart failure-associated key modules.

3.3. Identification of shared and key genes in COVID-19-associated heart failure

The hub genes of the heart failure-associated key module were screened out according to the criteria mentioned in the preceding method. Then, the common genes were obtained by intersecting the COVID-19-associated module genes with the heart failure-associated module genes. Consequently, totally eleven common genes were determined, as shown in Fig. 5A. To display their protein-protein interactions, a PPI network was generated based on the eleven common genes using the STRING website. After excluding unlinked proteins (namely WDR62, BLM, LINC00964, and ALKBH7, which did not have interaction with other proteins), seven pairs were obtained (Supplementary Fig. S1). A gene network cluster was identified exploiting MCODE analysis as seen in

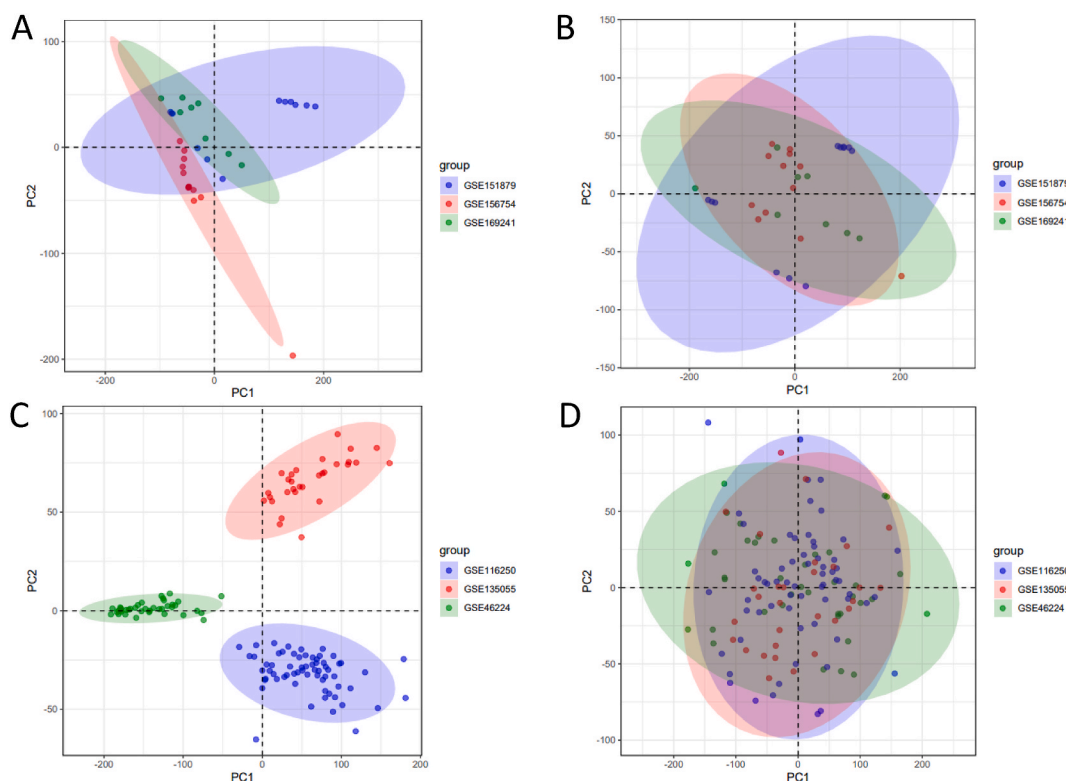


Fig. 2. PCA of before and after elimination of batch effect for all samples from the COVID-19 and heart failure datasets. (A, B) Represent the distribution of COVID-19 samples before and after elimination of batch effect, respectively. (C, D) Represent the distribution of heart failure samples before and after eliminating the batch effect, respectively.

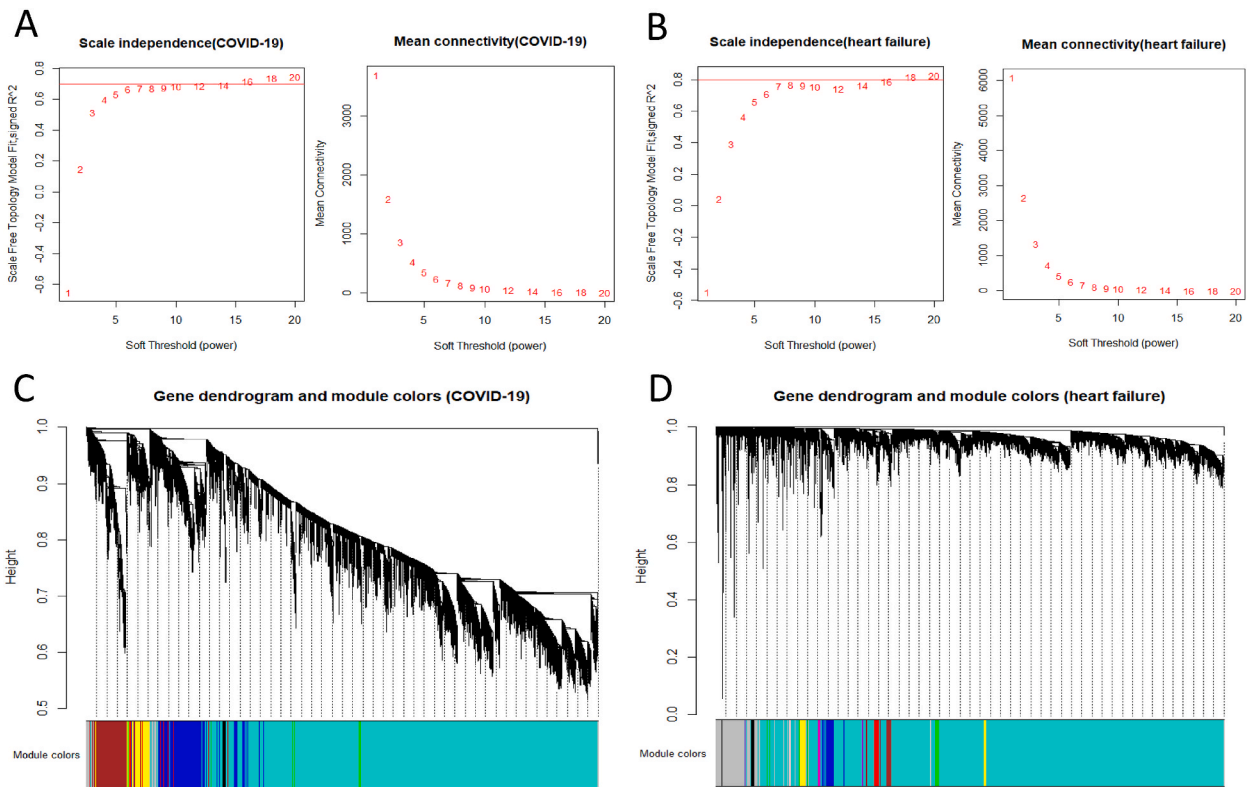


Fig. 3. Construction of weighted co-expression network for COVID-19 and heart failure-related datasets. (A, B) Network topology analysis of different soft threshold power. The effect of soft threshold power on the scale-free topology fit index is depicted in the left. The effect of soft threshold power on mean connectivity is depicted in the right. (C, D) Dendrograms of genes acquired by mean linkage hierarchical clustering. The allocation of modules decided by Dynamic Tree Cutting is displayed in the colored rows below the dendrogram.

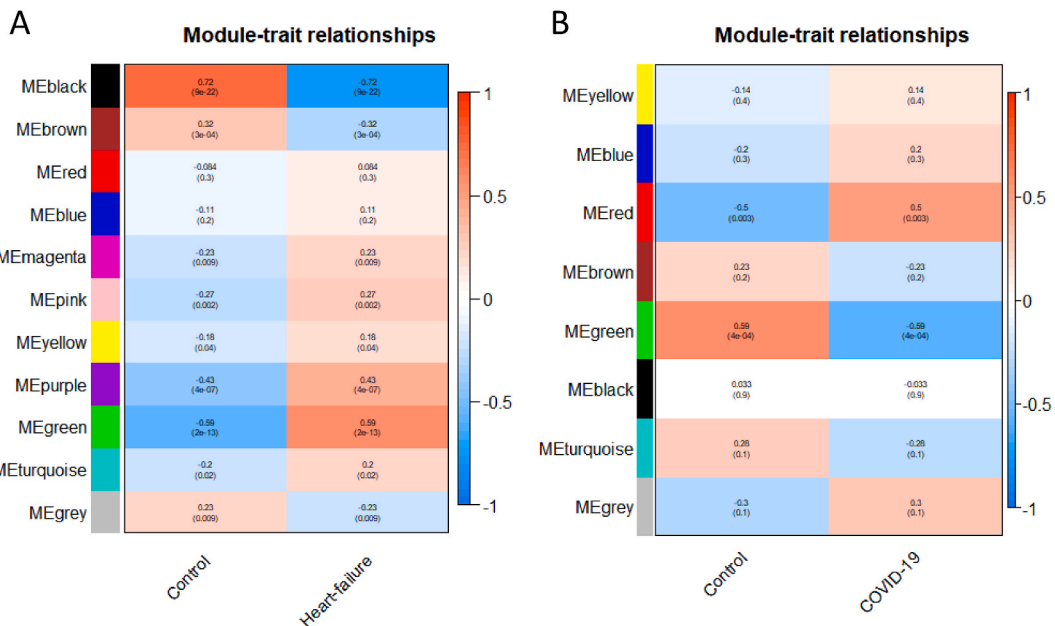


Fig. 4. Module-trait relationships. A, B. Each column represents a clinical feature (COVID-19 or heart failure and control), and each row denotes an ME. The correlation coefficient and P-value are contained in each cell. ME: module eigengene.

Fig. 5B, including PYGM, ALPK3, XIRP2, and FNDC5 key genes. Additionally, PYGM and BLM were obtained by intersecting the hub genes of heart failure-associated key module with the common genes, indicating that the two genes are more vital than additional shared genes in these biological processes of COVID-19-associated heart failure. Consequently, PYGM and BLM have been determined as key genes implicated in COVID-19-associated heart failure.

3.4. Functional enrichment analysis on shared genes of COVID-19-associated heart failure

We performed GO and KEGG enrichment analyses on shared COVID-19-associated heart failure genes to explore the potential biological process of COVID-19-associated heart failure. In respect of the common genes implicated in COVID-19-associated heart failure, the GO terms of biological process indicated that they were mainly enriched in cardiac muscle tissue morphogenesis, carbohydrate transmembrane transporter activity, positive regulation of DNA damage response, response to muscle stretch, negative regulation of DNA biosynthetic process, myoblast differentiation, and response to muscle activity. According to cellular components, relevant genes were mainly concentrated in the filamentous actin, precatalytic spliceosome, U5 snRNP, precatalytic spliceosome, stress fiber, peroxisomal membrane, catalytic step 2 spliceosome, spindle pole, Z disc, and centriole. In regard to molecular function, the common genes were mainly enriched in titin binding, alpha-actinin binding, R-SMAD binding, RNA polymerase II transcription coactivator activity, dioxygenase activity, RNA polymerase II transcription factor binding, p53 binding, pyridoxal phosphate binding, and nucleotide binding (Fig. 6A). Moreover, KEGG terms were enriched in starch and sucrose metabolism, homologous recombination, Fanconi anemia pathway, glucagon signaling pathway, insulin resistance, insulin signaling pathway, and necroptosis (Fig. 6B).

4. Discussion

- (1) In this research, we utilized the WGCNA package to explore the possible biological processes as well as crucial genes related to COVID-19 heart failure. Eleven shared genes were discovered in COVID-19- as well as heart failure-associated key modules, suggesting that they are the most probably to have several biological functions in COVID-19-associated heart failure. According to GO enrichment results, we found that the shared genes were predominantly related to cardiac muscle tissue morphogenesis, carbohydrate transmembrane transporter activity, positive regulation of DNA damage response, response to muscle stretch, negative regulation of DNA biosynthetic process, myoblast differentiation, and response to muscle activity. Additionally, these common genes were basically enriched in starch as well as sucrose metabolism, homologous recombination, Fanconi anemia pathway, glucagon signaling pathway, insulin resistance, insulin signaling pathway, and necroptosis. Moreover, studies in humans and animal models have revealed that heart failure is associated with generalized insulin resistance [23]. According to our enrichment results, we also found that these common genes were enriched in insulin resistance, indicates that insulin resistance may be associated with COVID-19-related heart failure.
- (2) There may be some possible limitations in this study. First, the potential two key targets in COVID-19-associated heart failure that we identified may require experimental validation to better support our findings. Second, the datasets do not contain relevant information such as co-morbidity and co-medications, and cannot be analyzed to explore the clinical relevance. Despite its preliminary character, this study can clearly indicate further insight into possible interventional and therapeutic targets.
- (3) Previous study has found that the OAS gene family which is associated with the antiviral immune responses of COVID-19 is highly expressed in both SARS-CoV-2 infected cardiomyocytes and failing hearts acting as an important mediator of HF in COVID-19 [24]. The OAS gene family encode interferon (IFN)-induced antiviral proteins. Recent study has indicated cardiac SARS-CoV-2 infection is associated with pro-inflammatory transcriptomic alterations [25]. These studies provide further investigations on SARS-CoV-2 infection may regulate the heart failure-associated genes. In our study, it is notable that PYGM and BLM were revealed to be the key genes for COVID-19-associated heart failure, indicating that they display a key part in COVID-19-associated heart failure. PYGM (cardiomyocyte-related muscle glycogen phosphorylase) is a protein-coding gene. which catalyzes and regulates the breakdown of glycogen to glucose-1-phosphate during glycogenolysis. This metabolic pathway is necessary for the generation of ATP during physical activity [26]. Briefly, it plays a central role in maintaining cellular and organismal glucose homeostasis. BLM (BLM RecQ Like Helicase) is a protein coding gene. Among its related pathways are homologous DNA pairing and strand exchange and resolution of D-loop structures through holliday junction intermediates [27]. It is an ATP-dependent DNA helicase that unwinds single- and double-stranded DNA in a 3'-5' direction, participates in DNA replication and repair [28,29]. ALPK3 (Alpha Kinase 3) is a protein coding gene, which predicted to enable ATP binding activity, protein serine kinase activity, and predicted to be involved in cardiac muscle cell development, implicated in hypertrophic cardiomyopathy. Moreover, cardiomyopathy was observed in ALPK3 deficient mice, which were otherwise normal phenotypically [30]. The ALPK3 signaling pathway and its implications on HF might provide insight to new therapeutic chances [31]. FNDC5 (Fibronectin Type III Domain Containing 5) is a gene that codes glycosylated transmembrane protein [32]. Previous findings suggest that FNDC5 could preserve mitochondrial function, attenuate oxidative damage and cell apoptosis [33]. In addition, recent studies also indicated that FNDC5 was involved in the regulation of several cardiovascular diseases, such as atherosclerosis, myocardial ischemia, and cardiac hypertrophy [34]. Xirp2 encodes xin actin-binding repeat containing 2, a muscle-specific actin binding protein, which is highly expressed in human heart tissues [35]. Several studies have discovered the role of Xirp2 on cardiac morphology and function. Additionally, Mutations in Xin loci are reported in different types of heart failure [36].
- (4) Although COVID-19 was originally considered a respiratory disease, it has rapidly become clear that a multiorgan involvement was common, especially the heart usually represents a target organ as well as patients may develop heart failure. Notably, the

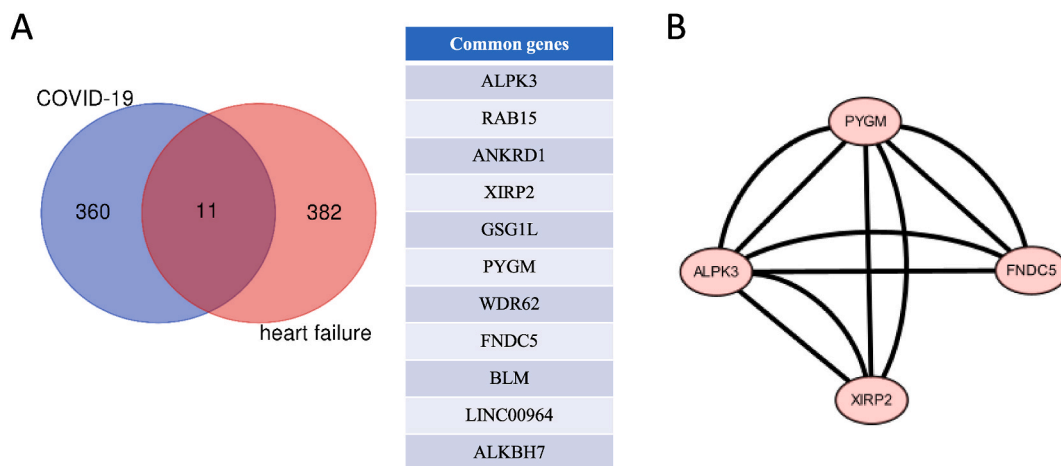


Fig. 5. Identification of common genes of COVID-19-related heart failure. A. Venn diagram of common genes in COVID-19-related crucial modules and heart failure-related crucial module. B. MCODE analysis results.

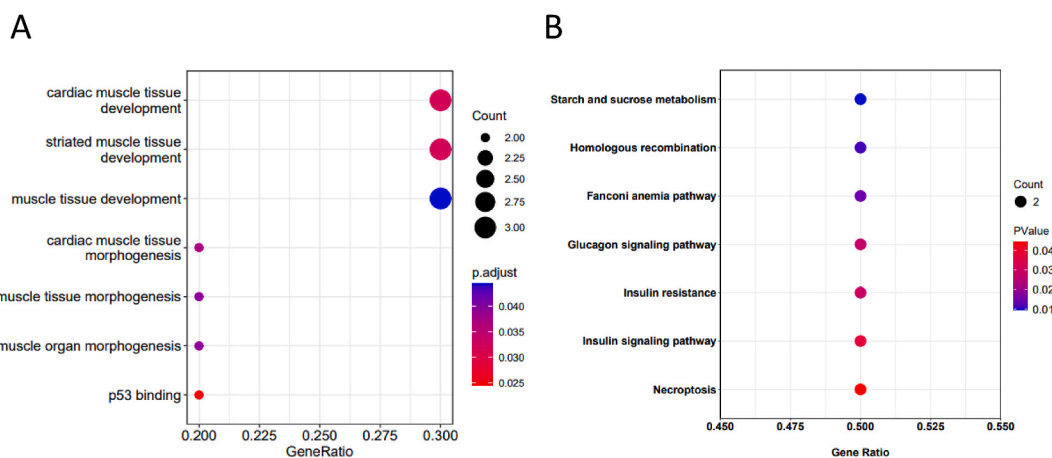


Fig. 6. The results of functional analysis of common genes. A. Gene Ontology enrichment analysis; B. Kyoto Encyclopedia of Genes and Genomes enrichment analysis.

connection between COVID-19 and heart failure is more complex [37–40]. Firstly, a risk element for a more serious clinical course of COVID-19 is history of heart failure. Furthermore, COVID-19-related myocardial damage may cause heart failure. In the present study, we performed bioinformatics analysis to explore the potential biological processes and key targets that might be implicated in the progression of COVID-19-associated heart failure, contributing to further insight into possible interventional and therapeutic targets of COVID-19-related heart failure. However, further investigations are required to define the precise molecular mechanism of key targets in COVID-19-related heart failure for fully understanding and appropriately apply in cardiovascular disease and respiratory disease.

5. Conclusions

The present study was designed to determine the underlying biological processes and key targets in COVID-19-related heart failure. For this task, totally eleven shared genes possibly be participated in several processes of COVID-19-associated heart failure via their involvement in starch and sucrose metabolism, homologous recombination, Fanconi anemia pathway, and insulin resistance. In addition, PYGM and BLM possibly be viable intervention targets for COVID-19-associated heart failure.

Author contribution statement

Jia Li: Conceived and designed the experiments; Performed the experiments; Analyzed and interpreted the data; Contributed reagents, materials, analysis tools or data; Wrote the paper.

Zhifu Guo: Conceived and designed the experiments. Contributed reagents, materials, analysis tools or data

Xiaowei Song: Conceived and designed the experiments.

Data availability statement

Data included in article/supp. material/referenced in article.

Declaration of competing interest

The authors declare that they have no known competing financial interests or personal relationships that could have appeared to influence the work reported in this paper.

Appendix A. Supplementary data

Supplementary data to this article can be found online at <https://doi.org/10.1016/j.heliyon.2023.e18575>.

References

- [1] C. Wang, P.W. Horby, F.G. Hayden, GEJTI Gao, A novel coronavirus outbreak of global health concern 395 (10223) (2020) 470–473.
- [2] L.T. Cowan, P.L. Lutsey, J.S. Pankow, K. Matsushita, J. Ishigami, Lakshminarayan KjjotAHA, Inpatient and outpatient infection as a trigger of cardiovascular disease, the ARIC study 7 (22) (2018), e009683.
- [3] M. Madjid, C.C. Miller, V.V. Zarubaev, I.G. Marinich, O.I. Kiselev, Y.V. Lobzin, A.E. Filippov, Casscells III, Swjehj, Influenza epidemics and acute respiratory disease activity are associated with a surge in autopsy-confirmed coronary heart disease death, results from 8 years of autopsies in 34 892 subjects 28 (10) (2007) 1205–1210.
- [4] J.-F. Dhainaut, Y.-E. Claessens, J. Janes, Nelson DRJCID, Underlying disorders and their impact on the host response to infection 41 (Supplement_7) (2005) S481–S489.
- [5] M. Madjid, P. Safavi-Naeini, S.D. Solomon, Vardeny OJJc, Potential effects of coronaviruses on the cardiovascular system: a review 5 (7) (2020) 831–840.
- [6] J.A. Fried, K. Ramasubbu, R. Bhatt, V.K. Topkara, K.J. Clerkin, E. Horn, L. Rabbani, D. Brodie, S.S. Jain, A.J.J.C. Kirtane, The variety of cardiovascular presentations of COVID-19 141 (23) (2020) 1930–1936.
- [7] F. Bader, Y. Manla, B. Atallah, Starling Rchfr, Heart failure and COVID-19 26 (1) (2021) 1–10.
- [8] E. Driggin, M.V. Madhavan, B. Bikdeli, T. Chuich, J. Laracy, G. Biondi-Zoccai, T.S. Brown, C. Der Nigoghossian, D.A. Zidar, Haythe JJJotACoc: cardiovascular considerations for patients, health care workers, and health systems during the COVID-19 pandemic 75 (18) (2020) 2352–2371.
- [9] J.T. Leek, W.E. Johnson, H.S. Parker, A.E. Jaffe, J.D.J.B. Storey, The sva package for removing batch effects and other unwanted variation in high-throughput experiments 28 (6) (2012) 882–883.
- [10] J.T. Leek, JDJPg Storey, Capturing heterogeneity in gene expression studies by surrogate variable analysis 3 (9) (2007) e161.
- [11] J.T. Leek, Storey JDJPotNAoS, A general framework for multiple testing dependence 105 (48) (2008) 18718–18723.
- [12] J.T. Leek, R.B. Scharpf, H.C. Bravo, D. Simcha, B. Langmead, W.E. Johnson, D. Geman, K. Baggerly, Irizarry RAJNRG, Tackling the widespread and critical impact of batch effects in high-throughput data 11 (10) (2010) 733–739.
- [13] P. Langfelder, SJBb Horvath, WGCNA: an R package for weighted correlation network analysis 9 (1) (2008) 1–13.
- [14] Raghov Rjtim, An ‘omics’ perspective on cardiomyopathies and heart failure 22 (9) (2016) 813–827.
- [15] S. Chen, Y. Zhou, Y. Chen, J.J.B. Gu, fastp: an ultra-fast all-in-one, FASTQ preprocessor 34 (17) (2018) i884–i890.
- [16] S. Andrews, FastQC: a quality control tool for high throughput sequence data, in: Babraham Bioinformatics, Babraham Institute, Cambridge, United Kingdom, 2010.
- [17] P. Ewels, M. Magnusson, S. Lundin, M.J.B. Källér, MultiQC: summarize analysis results for multiple tools and samples in a single report 32 (19) (2016) 3047–3048.
- [18] A. Dobin, C.A. Davis, F. Schlesinger, J. Drenkow, C. Zaleski, S. Jha, P. Batut, M. Chaisson, T.R.J.B. Gingeras, Star, ultrafast universal RNA-seq aligner 29 (1) (2013) 15–21.
- [19] Y. Liao, G.K. Smyth, W.J.B. Shi, featureCounts: an efficient general purpose program for assigning sequence reads to genomic features 30 (7) (2014) 923–930.
- [20] M. Carlson, S. Falcon, H. Pages, NJRpv Li, org. Hs. eg. db, 2019, Genome wide annotation for Human 2 (0) (2018).
- [21] B. Demchak, D. Otasek, A.R. Pico, G.D. Bader, K. Ono, B. Settle, E. Sage, J.H. Morris, W. Longabaugh, C.J.F. Lopes, The Cytoscape Automation app article collection 7 (800) (2018) 800.
- [22] T. Wu, E. Hu, S. Xu, M. Chen, P. Guo, Z. Dai, T. Feng, L. Zhou, W. Tang, L.J.T.I. Zhan, clusterProfiler 4.0: A universal enrichment tool for interpreting omics data 2 (3) (2021), 100141.
- [23] M. Velez, S. Kohli, Sabbah Hnjhr, Animal models of insulin resistance and heart failure 19 (2014) 1–13.
- [24] L.-J. Gao, Z.-M. He, Y.-Y. Li, R.-R. Yang, M. Yan, X. Shang, Cao J-MjjoTM, Role of OAS gene family in COVID-19 induced heart failure 21 (1) (2023) 1–19.
- [25] H. Bräuninger, B. Stoffers, A.D. Fitzek, K. Meißner, G. Aleshcheva, M. Schweizer, J. Weimann, B. Rotter, S. Warnke, Edler Cjcr, Cardiac SARS-CoV-2 infection is associated with pro-inflammatory transcriptional alterations within the heart 118 (2) (2022) 542–555.
- [26] S. Gautron, D. Daegelen, F. Mennecier, D. Dubocq, A. Kahn, Dreyfus J-Cjyjoci, Molecular mechanisms of McArdle’s disease (muscle glycogen phosphorylase deficiency), RNA and DNA analysis 79 (1) (1987) 275–281.
- [27] J.K. Karow, R.K. Chakraverty, Hickson IDJJoBC, The Bloom’s syndrome gene product is a 3’-5’ DNA helicase 272 (49) (1997) 30611–30614.
- [28] G. Langland, J. Elliott, Y. Li, J. Creaney, K. Dixon, Groden Jjcr, The BLM helicase is necessary for normal DNA double-strand break repair 62 (10) (2002) 2766–2770.
- [29] A.V. Nimonkar, J. Genschel, E. Kinoshita, P. Polaczek, J.L. Campbell, C. Wyman, P. Modrich, S.C.J.G. Kowalczykowski, development: BLM–DNA2–RPA–MRN and EXO1–BLM–RPA–MRN constitute two DNA end resection machineries for human DNA break repair 25 (4) (2011) 350–362.
- [30] I. Van Slijghenhorst, Z. Ding, Z.-Z. Shi, R. Read, G. Hansen, PJVp Vogel, Cardiomyopathy in α -Kinase 3 (ALPK3)–deficient mice 49 (1) (2012) 131–141.
- [31] S. Guo, Y. Yang, W. Qian, Y. Yao, G. Zhou, L. Shen, JJJoB. Zhou, M. Toxicology, MicroRNA-384-5p Protects against Cardiac Hypertrophy via the ALPK3 Signaling Pathway, 2022, e23093.
- [32] P. Boström, J. Wu, M.P. Jedrychowski, A. Korde, L. Ye, J.C. Lo, K.A. Rasbach, E.A. Boström, J.H. Choi, J.Z.J.N. Long, A, PGC1- α -dependent myokine that drives brown-fat-like development of white fat and thermogenesis 481 (7382) (2012) 463–468.
- [33] L. Ling, D. Chen, Y. Tong, Y.-H. Zang, X.-S. Ren, H. Zhou, X.-H. Qi, Q. Chen, Y.-H. Li, Kang Y-Mjijoh, F, Ibronectin type III domain containing 5 attenuates NLRP3 inflammasome activation and phenotypic transformation of adventitial fibroblasts in spontaneously hypertensive rats 36 (5) (2018) 1104–1114.

- [34] R.-L. Li, S.-S. Wu, Y. Wu, X.-X. Wang, H.-Y. Chen, J.-j. Xin, H. Li, J. Lan, K.-Y. Xue, XJJoM. Li, et al., Irisin alleviates pressure overload-induced cardiac hypertrophy by inducing protective autophagy via mTOR-independent activation of the AMPK-ULK1 pathway 121 (2018) 242–255.
- [35] J. Otten, P.F. van der Ven, P. Vakeel, S. Eulitz, G. Kirfel, O. Brandau, M. Boesl, J.W. Schrickel, M. Linhart, Hayeß Kjcr, Complete loss of murine Xin results in a mild cardiac phenotype with altered distribution of intercalated discs 85 (4) (2010) 739–750.
- [36] Q. Wang, J.L.-C. Lin, A.J. Erives, C.-I. Lin, Lin Jj-Cjiroc, Biology m: new insights into the roles of Xin repeat-containing proteins in cardiac development, function, and disease 310 (2014) 89–128.
- [37] D. Tomasoni, L. Italia, M. Adamo, R.M. Inciardi, C.M. Lombardi, S.D. Solomon, Metra Mjejohf, COVID-19 and heart failure: from infection to inflammation and angiotensin II stimulation, Searching for evidence from a new disease 22 (6) (2020) 957–966.
- [38] Y.-Y. Zheng, Y.-T. Ma, J.-Y. Zhang, XJNrc Xie, COVID-19 and the cardiovascular system 17 (5) (2020) 259–260.
- [39] P.P. Liu, A. Blet, D. Smyth, H.J.C. Li, The science underlying COVID-19: implications for the cardiovascular system 142 (1) (2020) 68–78.
- [40] T.-Y. Xiong, S. Redwood, B. Prendergast, MJEhj Chen, Coronaviruses and the Cardiovascular System: Acute and Long-Term Implications, 2020.